Measurement of Raman Optical Activity with High-Frequency Polarization Modulation

Carin R. Lightner,[†] Daniel Gisler,[‡,§] Stefan A. Meyer,[†] Hannah Niese,[†] Robert C. Keitel,[†] and David J. Norris[,†]*

[†]Optical Materials Engineering Laboratory, Department of Mechanical and Process Engineering, ETH Zurich, 8092 Zurich, Switzerland

[‡]Istituto Ricerche Solari Locarno (IRSOL), 6605 Locarno-Monti, Switzerland

[§]Università della Svizzera italiana (USI), 6605 Locarno-Monti, Switzerland

ABSTRACT. Many chiroptical spectroscopic techniques have been developed to detect chirality in molecular species and probe its role in biological processes. Raman optical activity (ROA) should be one of the most powerful methods, as ROA yields vibrational and chirality information simultaneously and can measure analytes in aqueous and biologically relevant solvents. However, despite its promise, the use of ROA has been limited, largely due to challenges in instrumentation. Here, we report a new approach to ROA that exploits high-frequency polarization modulation. High-frequency polarization modulation, usually implemented with a photoelastic modulator (PEM), has long been the standard technique in other chiroptical spectroscopies. Unfortunately, the need for simultaneous spectral and polarization resolution has precluded the use of PEMs in ROA instruments. We combine a specialized camera system (the Zurich Imaging Polarimeter, or ZIMPOL) with PEM modulation to perform ROA measurements. We demonstrate performance similar to the current standard in ROA instrumentation while reducing complexity and polarization artifacts. This development should aid researchers in exploiting the full potential of ROA for chemical and biological analysis.

INTRODUCTION

An object is chiral when it is not superimposable on its mirror image. Chirality, or handedness, exists throughout the natural world, *e.g.* in physiology, crystalline solids, and subatomic particles.[1] In chemistry, the left- and right-handed forms of a chiral molecule are called enantiomers. Although they have the same molecular formula, the lack of symmetry in the arrangement of the atoms can lead to completely different effects in the human body.[2] Therefore, chirality is critical for the development of pharmaceutics and in furthering our understanding of biological processes.[3]

While the importance of molecular chirality is clear, spectroscopic differentiation of enantiomers is not always straightforward. Chiroptical techniques exploit the fact that enantiomers interact differently with circularly polarized light (CPL), which itself exists as both a right- (RH) and left-handed (LH) form. Differences in the interaction of a chiral molecule with RH- and LH-CPL are referred to as optical activity. It can be observed in virtually any optical phenomenon, from absorption to fluorescence to scattering.[4] The effect can be measured by detecting the difference in intensity of the observed phenomenon when measured with RH- and LH-CPL. For instance, optical activity in absorption can be quantified by the difference in intensity of RH-CPL transmitted through the sample ($I_{\mathrm{R}}^{\mathrm{t}}$) *versus* LH-CPL ($I_{\mathrm{L}}^{\mathrm{t}}$). More generally, optical activity for any optical phenomena is typically given in terms of the dissymmetry factor, defined as the normalized quantity $\Delta = (I_{\mathrm{R}} - I_{\mathrm{L}})/(I_{\mathrm{R}} + I_{\mathrm{L}})$, where I_{R} and I_{L} represent signal intensities for the specific optical phenomenon probed with RH- and LH-CPL, respectively.

Optical activity is most commonly measured in absorption (known as circular dichroism) and fluorescence (known as circularly polarized luminescence). However, optical activity in scattering can potentially provide more detailed information. For example, Raman scattering from chiral molecules can lead to Raman optical activity (ROA).[4] In traditional Raman

spectroscopy, incident light is inelastically scattered from molecules in the sample. The spectral shift from the incident wavelength for each Raman line gives information about the vibrational modes of the molecule. In ROA, the same scattering is measured for RH- and LH-CPL. The difference in scattered intensity ($I_R^s - I_L^s$) is measured, leading to spectra for two molecular enantiomers that exhibit mirror symmetry in the ROA peaks about the wavelength axis.[5] Together, this information can help identify the molecule and its handedness. In addition, ROA can be used to more easily differentiate molecules with several chiral centers and even elucidate tertiary structural information of large biomolecules.[6,7] Other advantages of ROA include its applicability to virtually any chiral molecule and its suitability to measurements in aqueous solutions (as water exhibits weak Raman scattering). However, the main disadvantage of ROA is that it is an extremely weak effect. This leads to instrumentation challenges when optical polarization states must be determined with extremely high precision.

Because the dissymmetry factors in ROA are, at most, on the scale of 10^{-3}, the LH- and RH-CPL must be separated with a precision exceeding this. In addition, because the fundamental effect (Raman scattering) itself is relatively weak, the measurement must be done in a relatively "photon-starved" environment. In most chiroptical spectroscopy techniques, a linear polarizer and a variable phase modulator, typically a photoelastic modulator (PEM), are used to create CPL in the excitation path or to measure the circular component in the emitted light in the collection path.[8-9] PEMs rely on photoelasticity, *i.e.* the change in optical properties of a material under mechanical deformation to create a variable retarder for the optical phase. A strain is induced in the PEM material, leading to a desired retardation.[10] While other devices such as Pockels cells or liquid crystal retarders (LCR) can also be used as variable phase retarders, PEMs have several significant advantages. They produce reliable phase retardations, have large optical apertures, are stable over long periods of time, and can modulate at high

frequencies (20–84 kHz).[11] This is in contrast to LCRs, which exhibit hysteresis, and Pockels cells, which have small (< 10 mm) optical apertures.[11-12]

Another advantage of PEMs is that they can be combined with a lock-in amplifier to extract polarization information with high signal to noise.[11,13] However, this approach must then use fast point detectors to collect the scattered light. Such detectors can be synchronized with the high-frequency modulation of the PEM. This presents a challenge for ROA, because a spectrum of the scattered light should be obtained. Ideally, one would like to use a spectrometer to disperse the signal onto a charge-coupled-device (CCD) camera and obtain the spectral information in parallel. Unfortunately, read out of a CCD chip is too slow to be coupled to the high-speed modulation of the PEM. Consequently, one instead scans a monochromator, collecting one wavelength at a time with the fast point detector. This approach, which, by necessity, was used in early ROA instruments, leads to instrumental artifacts and prohibitively long measurement times that impede the general use of ROA.[14-15]

Here, we present a different route that exploits fast polarization modulation with a PEM to collect ROA spectra. We employ a unique optical detector, a Zurich Imaging Polarimeter (ZIMPOL) system, and combine it with a PEM. The ZIMPOL system is built around a CCD imaging detector, but it allows the modulation speed of the PEM to be decoupled from the slow CCD readout speed. This is achieved by using a partially masked CCD detector and shifting the charges from the unmasked area of the CCD to the masked areas.[11,16] The shifting of the charges can be synchronized with the PEM such that the different polarization states are sorted onto different rows of the CCD. Meanwhile, a grating in the detection path disperses the wavelength information onto different columns of the CCD. The CCD output can then be processed to obtain ROA spectra. The use of a PEM means that polarization artifacts inherent in other forms of polarization modulation, such as LCRs, can be avoided. Consequently, the stability and reliability of PEMs, which have long been preferred for polarization modulation

in other commercial chiroptical measurement systems, can be exploited in ROA measurements. After describing our new apparatus, we compare it to other more traditional ROA instruments. We find that our first-generation device offers similar performance while greatly reducing instrument complexity. Thus, we demonstrate a new approach to ROA instrumentation that can potentially bring ROA spectrometers to the level of other chiroptical techniques.

EXPERIMENTAL SECTION

ROA can be measured either by modulating the polarization of the incident laser light (ICP) or by measuring the circular component in the scattered light (SCP).[17] The ROA spectra from ICP and SCP measurements should be identical.[4] Indeed, this has been confirmed by several experimental reports.[12,18] The choice between SCP and ICP is then one of experimental convenience. For the construction of our instrument (see Figure 1), the SCP configuration was selected to facilitate comparison with other reported ROA data, which were collected using SCP. Our apparatus should work equally well with ICP, in which case, the PEM would be used to modulate the incident laser beam.

The second choice in the construction of our ROA instrument was the angle from which to collect the scattered light. In the literature, back-scattering, 90-degree-scattering, forward-scattering, and so-called "magic-angle-scattering" have all been used.[8] Each of these configurations leads to different contributions from the optical-activity tensors and therefore different ROA spectra.[19] This choice is therefore more consequential than the choice of SCP *versus* ICP. Back-scattering is generally preferred because it exhibits higher dissymmetry due to lower contributions from standard Raman scattering. The experimental realization of SCP-ROA with the back-scattering configuration is, however, challenging. Traditional optical techniques such as using a beam-splitting cube to excite and collect in the same path are not possible because they introduce polarization artifacts. To avoid this while still using back-scattering, the laser can be launched into the sample path *via* two small right-angle prism

mirrors.[12,20] Unfortunately, this approach, which has been employed in several successful ROA instrument variations, introduces a large amount of birefringence and alignment sensitivity.

Therefore, we chose forward-scattering instead. This configuration has been previously demonstrated experimentally and, while fewer features appear in the resulting ROA spectra, forward-scattering is still able to easily distinguish enantiomers.[21-22] Constructing the instrument in forward-scattering also allows all of the polarization conditioning optics to be in the same plane, as shown in Figure 1. This reduces polarization artifacts and alignment issues. A small 3 mm right-angle silver mirror is still used, but now it deflects the laser beam out of the signal path after interacting with the sample. Therefore, this optical element does not affect the polarization of forward-scattered light that is collected.

The main advantage of our instrument is its use of a PEM to separate the polarization states in the collected signal. Invented in 1966, PEMs exploit the inverse piezoelectric effect in optical materials to produce strain-induced birefringence using an electrical signal. This allows PEMs to act as high-frequency variable phase retarders. The retardation follows a sinusoidal pattern where the maximum retardation can be set by the PEM electronics. Our PEM (Hinds Instruments, II/FS42) operates at 42 kHz and is set so that at its maximum retardation it is approximately a quarter-wave plate. At this point, the CPL incident on the PEM is converted to linearly polarized light at ±45° to the PEM optical axis. (+ is defined as a clockwise rotation looking in the direction of light propagation.) This light then passes through a linear polarizer set at +45° to the PEM optical axis. The polarization state in the beam incident on the PEM is therefore converted after the linear polarizer to a beam with sinusoidally varying intensity at the PEM operating frequency.

Unfortunately, it has not been possible to use high-frequency modulators such as PEMs in ROA measurements because of the difficulty of coupling a modulator at > 1 kHz to a CCD detector. The detector read-out speed is too slow to allow high-frequency polarization

modulation. This has limited PEMs to setups with high-speed point detectors. Our instrument avoids this problem with the use of the ZIMPOL detection system.[11,23-24] ZIMPOL utilizes a partially masked CCD and then synchronizes the movement of the charges between rows of the CCD with the PEM, effectively decoupling the speed of the polarization modulation from the read-out speed of the camera.[16] The ZIMPOL system used in our ROA instrument masks three of every four pixel rows on the CCD (which has 560 pixel rows total) and then moves the charges between rows such that during one PEM modulation cycle the signal is distributed over the four pixel rows in time. This allows the LH- and RH-CPL spectra to be separated onto rows 1 and 3 and the 45° linear polarization spectra onto rows 2 and 4 (see Figure S1 in the Supporting Information). Additionally, a microlens array is mounted in front of the mask so that the optical signal is efficiently channeled through the holes in the mask (see inset in Figure 1).

Our overall instrument design (Figure 1) was heavily influenced by Hug *et al.*[21-22] For excitation, a 2 W 532 nm continuous-wave (cw) laser (Coherent, Verdi 2W) is sent through a Glan-Taylor laser prism with an extinction ratio of 1:100,000 to improve the polarization purity of the input beam. This is followed by "linear rotators," which consist of two counter-rotating zero-order half-wave plates.[25] These are rotated at approximately 300 rpm in custom-made rotating mounts.[25] Such rotation is necessary because a significant source of artifacts in ROA measurement is birefringence in the excitation path. By rotating the plane of linear polarization over all angles, depolarized light is created on the time scale of a single spectral acquisition, effectively canceling out any birefringence in the excitation path. Additionally, two half-wave plates can be moved in and out of the optical path before and after the sample. These act as circular converters (CC1 and CC2, Figure 1) and are part of the virtual enantiomer correction scheme,[25] which is discussed in detail in the next section.

Light is focused onto the sample using a 25.4 mm diameter lens with a 100 mm focal distance. The sample is held in either a glass vial or a custom-made sample holder. After the sample, the scattered signal is collected using a 25.4 mm diameter lens with a 30 mm focal distance, while the transmitted laser beam is deflected from the center of the path into a beam dump using a 3 mm right-angle mirror positioned in the center of the lens using a custom mount. When in use, the second circular converter (CC2) is positioned behind the beam deflector, after which the light is incident on the PEM. As mentioned above, after the PEM a linear polarizer is set at 45° to the PEM optical axis, followed by a Rayleigh filter (Iridian, Dielectric Super Notch Plus Filter). The signal is then focused onto a 50 μm slit and launched into an Andor Holospec high-throughput spectrometer, after which it is measured by the ZIMPOL camera system. Detailed information about all of our optical components, including manufacturer and part number, are included in the Supporting Information in Table S1. The sources for our chemicals are listed in Table S2.

RESULTS AND DISCUSSION

Calibration and Control Measurements. To evaluate the performance of our ROA spectrometer we measured experimental variables that have already been reported for comparable instruments. For this, we identified the depolarization ratio (*DR*) and the degree of circularity (*DOC*) of carbon tetrachloride (CCl_4) as useful parameters for which data exists in the literature.[12,21] CCl_4 is an achiral molecule, and has no ROA signal. However, the vibrational modes in CCl_4 are highly polarized, meaning that because of anisotropic invariants in the standard Raman tensor, they exhibit strong differences in their response to perpendicular linear polarization states.[5] The level of polarization of a mode is quantified by the depolarization ratio (*DR*), defined as

$$DR(0^\circ,\ +45^{\circ,i}) = \frac{I^{s}_{+45}}{I^{s}_{-45}} = \frac{I^{s}_{\perp}}{I^{s}_{\parallel}} \quad (1)$$

The first term in the parentheses indicates the direction of the collected Raman-scattered light (0° is forward-scattering), and the second term, $+45^{\circ,i}$, indicates the polarization of the light incident on the sample, here at $+45^\circ$ with respect to the PEM optical axis. *DR* is calculated by dividing the intensities of perpendicular linear polarization states measured in the scattered light [indicated by I^s_{+45} (or $I^s_\perp$) and I^s_{-45} (or $I^s_\parallel$)]. A mode is considered polarized when[5]

$$0 < DR(0^\circ,\ +45^{\circ,i}) < \frac{3}{4} \tag{2}$$

The measurement of *DR* is useful for quantifying the precision of linear polarization that an optical setup can measure as well as its sensitivity to the amount of linear polarization in the incident path. The degree of circularity (*DOC*) measures the same tensor invariants but with incident circularly polarized light according to

$$DOC(0^\circ, I^i_R) = \frac{I^s_R - I^s_L}{I^s_R + I^s_L} \tag{3}$$

Here, I^s_R and I^s_L are the intensities of Raman-scattered RH- and LH-CPL, respectively. Figure 2 shows *DOC* (top), *DR* (center), and Raman spectra for CCl_4.

A second useful control is to compare the *DR* value measured with incident linearly polarized light to the calculated *DR* from the *DOC*. We can exploit the fact that *DOC* and *DR* are related by[5]

$$DR(0^\circ,\ +45^{\circ,i}) = \frac{1 - DOC(0^\circ, I^i_R)}{3 + DOC(0^\circ, I^i_R)} \tag{3}$$

where $DOC(0^\circ, I^i_R)$ is the degree of circularity in forward-scattering, measured with incident right-circularly polarized light.

By taking measurements of the *DR* and *DOC* on CCl_4 and comparing the values to those reported in the literature, the performance of the new ROA instrument can be evaluated. Because *DOC* and *DR* are normalized quantities, they can be easily compared across instruments, rather than the intensities and shapes of ROA spectra which depend strongly on the exact experimental set-up. The use of both measurements (*DOC* and *DR*) reveals how a

given instrument interacts with linear *versus* circularly polarized light, and since the separation of perpendicular linear polarization states is often much easier than the separation of opposite circularly polarized states, this also acts as a useful instrumental reference.

Table 1 compares measurements from our instrument (Z-ROA) to those from the instrument of Hug *et al.* as well as calculated values for two CCl_4 vibrational modes.[5,12] We find good agreement for the *DOC* values for both modes and relatively good agreement for *DR* measured and calculated at 316 cm^{-1}. The measured value for *DR* at the 460 cm^{-1} mode in this instrument is, however, much larger than expected (0.038 measured *versus* 0.002 calculated). This reflects the fact that this instrument, though able to measure linearly polarized light, is optimized for circularly polarized light. For modes that are almost completely polarized (like the 460 cm^{-1} mode in CCl_4), very little signal exists for one polarization state, reducing the signal-to-noise ratio and the measurement precision. Similarly, in the *DR* spectra in Figure 2, noise increases in the regions without peaks because two values with very low signals are being divided. In comparison, because *DOC* is the difference over the sum of the CPL, the values in regions with no features will always be close to zero because the total signal (*i.e.*, the denominator) will always be orders of magnitude larger than the difference signal.

The *DOC* is also a useful control measurement because it indicates which bands are strongly polarized (*DOC* close to 1 or −1). Strongly polarized modes tend to result in a circular signal that is the result not of the chirality of the molecule but the anisotropic invariants of the standard Raman scattering tensor. Figure 3 shows the forward-scattered ROA spectra for two achiral molecules, toluene and carbon tetrachloride, and compares these signals to the expected shot noise, which is calculated as the square root of the Raman signal.[21] Because the incident light is depolarized and the molecules are achiral, zero signal in the circular difference spectra is expected. For both molecules, the peaks in the ROA spectra are largely below the noise except those that correspond to strongly polarized modes, as indicated by the *DOC* spectra in

the top panel. Artifacts caused by strongly polarized modes are of even greater concern when measuring chiral molecules, and for this reason we show the *DOC* spectra in the top panel of each ROA measurement below. Modes that appear in the ROA spectra and are also strongly polarized, as indicated by the *DOC*, should always be closely examined. Additional control measurements, with varying laser powers and accumulation times, are shown in Figures S2-S5 in the Supporting Information.

ROA Measurements. Figure 4 shows ROA measurements for two chiral molecules (α-pinene and β-pinene). The β-pinene measurement was made in just 4 minutes while α-pinene required a longer measurement time (40 min) to achieve the desired resolution. Both α-pinene and β-pinene show mirror-image spectra for enantiomers, and the peaks are similar to those reported from other forward-scattering ROA instruments.[21-22] Because the goal of this study was to test whether it would be possible to measure SCP-ROA using a PEM in the scattered path, rather than compete with the commercially available ROA systems, larger measurement volumes (1 mL) were typically used. With further effort the sample volume could likely be reduced. Unlike other ROA instruments, our apparatus requires little to no re-alignment, and once the optical path is fixed the measurements are consistent. This is likely due to the simplified optical path that was achieved with forward-scattering and the stability and reliability of the PEM. ROA of limonene was also measured and is shown in Figure S6.

Virtual Enantiomer Scheme. Both measurements in Figure 4 were taken with two-phase correction, meaning that for each ROA spectrum a measurement was first taken without CC1 and CC2 in the optical path (see Figure 1) and then a second measurement was taken with CC1 and CC2 in the optical path. The two measurements are then subtracted from each other to remove any offsets caused by instrumentation. This scheme was introduced first by Hug *et al.* and is now widely used in most ROA instruments.[25] In our Z-ROA instrument, the only offsets present appear to be those generated from the strongly polarized modes.

Figure 5 shows measurements of β-pinene taken without phase correction (without CC1 and CC2 in the optical path), with 2-phase correction and with 4-phase correction. The 4-phase correction scheme consists of taking four separate measurements, with CC1 in, CC2 in, CC1 and CC2 in, and a final measurement with no half-wave plates in the path. The 4-phase measurement also corrects for the small discrepancies caused by the half-wave plates themselves.[25] The largest difference between the measurement without correction and with 2-phase and 4-phase correction is the flipping of the strongly polarized mode at 640 cm^{-1}. This suggests that the largest source of offsets in this instrument are those caused by the strongly polarized modes of the measured molecules. This appears to differ from other instruments where the virtual enantiomer scheme of Hug *et al.* corrected for larger offsets caused by birefringence in the optical path.[25] A possible reason for this is the use of forward-scattering which avoids the difficult beam deflection scheme. More investigation is needed to compare this instrument with others and understand the sources of the offsets in each.

CONCLUSION

In this work we have demonstrated that high-frequency modulation, in the form of a PEM, can be used to measure ROA. This was made possible by using the ZIMPOL system to couple the PEM modulation to a CCD detector. The performance of this newly developed ROA instrument was compared with previous reports through measurements of the depolarization ratio and the degree of circularity. Several achiral molecules were also measured to determine the influence of chiral artifacts and offsets. The development of ROA instrumentation has lagged behind those for other chiroptical techniques because of its high sensitivity to artifacts and its requirement for spectral resolution. The instrument developed here shows that the benefits of using highly stable PEMs for polarization modulation can now be applied to ROA, greatly simplifying instrumentation and reducing measurement artifacts.

ASSOCIATED CONTENT

Supporting Information

The Supporting Information is available free of charge on the ACS Publications website at DOI: 10.1021/xxxxxxx.

ZIMPOL description (Section S1), detailed list of all optical components (Section S2) and chemicals used (Section S3), additional control measurements (Section S4), and ROA spectra of limonene (Section S5)

AUTHOR INFORMATION

Corresponding Author

*Email: dnorris@ethz.ch

ORCID

Carin R. Lightner: 0000-0003-3132-0296

Stefan A. Meyer: 0000-0002-0271-0028

Hannah Niese: 0000-0002-5980-5386

Robert C. Keitel: 0000-0002-9412-8034

David J. Norris: 0000-0002-3765-0678

Funding

C.R.L. acknowledges support from the President of ETH Zurich.

Notes

The authors declare the following potential competing financial interest: C.R.L., D.G., and D.J.N. are seeking patent protection for the ideas in this work.

ACKNOWLEDGMENTS

We thank J. Stenflo for his support in putting us in contact with the ZIMPOL team. We would

also like to thank T. Bürgi and R. Brechbühler for helpful discussions. And finally, we are grateful to our collaborators at IRSOL and SUPSI for their help and support in installing and improving the ZIMPOL system for use in ROA including P. Steiner for his support with the ZIMPOL software systems.

REFERENCES

1. Mason, S., The Origin of Chirality in Nature. *Trends Pharmacol. Sci.* **1986**, *7,* 20-23.
2. Tokunaga, E.; Yamamoto, T.; Ito, E.; Shibata, N., Understanding the Thalidomide Chirality in Biological Processes by the Self-disproportionation of Enantiomers. *Sci. Rep.* **2018**, *8,* 17131.
3. Brooks, W. H.; Guida, W. C.; Daniel, K. G., The Significance of Chirality in Drug Design and Development. *Curr. Top. Med. Chem.* **2011**, *11,* 760-770.
4. Barron, L. D., *Molecular Light Scattering and Optical Activity*. Cambridge University Press: Cambridge, 2004.
5. Long, D. A., *The Raman Effect*. John Wiley and Sons LTD: West Sussex, 2002.
6. Bogaerts, J.; Desmet, F.; Aerts, R.; Bultinck, P.; Herrebout, W.; Johannessen, C., A Combined Raman Optical Activity and Vibrational Circular Dichroism Study on Artemisinin-Type Products. *Phys. Chem. Chem. Phys.* **2020**, *22,* 18014-18024.
7. Barron, L. D.; Zhu, F.; Hecht, L.; Tranter, G. E.; Isaacs, N. W., Raman Optical Activity: An Incisive Probe of Molecular Chirality and Biomolecular Structure. *J. Mol. Struct.* **2007**, *834,* 7-16.
8. Nafie, L. A., *Vibrational Optical Activity: Principles and Applications*. Wiley Online Library: Syracuse, 2011.
9. Poulikakos, L. V.; Gutsche, P.; McPeak, K. M.; Burger, S.; Niegemann, J.; Hafner, C.; Norris, D. J., Optical Chirality Flux as a Useful Far-Field Probe of Chiral Near Fields. *ACS Photonics* **2016**, *3,* 1619-1625.
10. Hipps, K. W.; Crosby, G. A., Applications of the Photoelastic Modulator to Polarization Spectroscopy. *J. Phys. Chem.* **1979**, *83,* 555-562.
11. Stenflo, J., Solar Polarimetry with ZIMPOL. *Mem. Soc. Astron. Ital.* **2007**, 183-190.
12. Hug, W.; Hangartner, G., A Novel High-Throughput Raman Spectrometer For Polarization Difference Measurements. *J. Raman Spectrosc.* **1999**, *30,* 841-852.

13. Kemp, J. C.; Barbour, M. S., A Photoelastic-Modulator Polarimeter at Pine Mountain Observatory. *Publ. Astron. Soc. Pac.* **1981**, *93,* 521.

14. Barron, L. D.; Buckingham, A. D., Rayleigh and Raman Optical Activity. *Annu. Rev. Phys. Chem.* **1975**, *26,* 381-396.

15. Barron, L. D.; Torrance, J. F.; Cutler, D. J., A New Multichannel Raman Optical Activity Instrument. *J. Raman Spectrosc.* **1987**, *18,* 281-287.

16. Povel, H.; Aebersold, H.; Stenflo, J. O., Charge-Coupled Device Image Sensor as a Demodulator in a 2-D Polarimeter with a Piezoelastic Modulator. *Appl. Opt.* **1990**, *29,* 1186-1190.

17. Barron, L. D.; Hecht, L.; McColl, I. H.; Blanch, E. W., Raman Optical Activity Comes of Age. *Mol. Phys.* **2004**, *102,* 731-744.

18. Spencer, K. M.; Freedman, T. B.; Nafie, L. A., Scattered Circular Polarization Raman Optical Activity. *Chem. Phys. Lett.* **1988**, *149,* 367-374.

19. Hecht, L.; Barron, L. D., An Analysis of Modulation Experiments for Raman Optical Activity. *Appl. Spectrosc.* **1989**, *44,* 483-491.

20. Hug, W., *Encyclopedia of Spectroscopy and Spectrometry (Third Edition).* Academic Press: 2017; p 881-890.

21. Haesler, J. Construction of a New Forward and Backward Scattering Raman Optical Activity Spectrometer and Graphical Analysis of Measured and Calculated Spectra for (R)-[$^2H_1$,$^2H_2$,$^2H_3$]-Neopentane. University of Fribourg, 2006.

22. Barron, L. D.; Hecht, L.; Gargaro, A. R.; Hug, W., Vibrational Raman Optical Activity in Forward Scattering: Trans-pinane and β-pinene. *J. Raman Spectrosc.* **1990**, *21,* 375-379.

23. Ramelli, R.; Balemi, S.; Bianda, M.; Defilippis, I.; Gamma, L.; Hagenbuch, S.; Rogantini, M.; Steiner, P.; Stenflo, J. O. In *ZIMPOL-3: A Powerful Solar Polarimeter*, 2010/07/1; p 77351Y.

24. Gandorfer, A. M.; Steiner, H. P. P. P.; Aebersold, F.; Egger, U.; Feller, A.; Gisler, D.; Hagenbuch, S.; Stenflo, J. O., Solar Polarimetry in the Near UV With the Zurich Imaging Polarimeter ZIMPOL II. *Astron. Astrophys.* **2004**, *422,* 703-708.

25. Hug, W., Virtual Enantiomers as the Solution of Optical Activity's Deterministic Offset Problem. *Appl. Spectrosc.* **2002**, *57,* 1-13.

	Raman Mode (cm^{-1})	Degree of Circularity	Calculated Depolarization Ratio	Measured Depolarization Ratio
Theoretical values[5]	316	−0.710	0.750	–
	460	0.960	0.010	–
Instrument of Hug *et al.*[12]	316	0.689	0.730	0.740
	460	−0.979	0.005	0.005
Z-ROA	316	−0.693	0.734	0.734
	460	0.994	0.002	0.038

Table 1. Comparison of the values of the degree of circularity (*DOC*), the measured depolarization ratio (*DR*), and the depolarization ratio calculated from the *DOC* for two Raman modes of CCl_4. The theoretical values are shown in the top two rows, then values measured from the back-scattering instrument of Hug *et al.*,[12] and finally values measured from our instrument (Z-ROA). The sign differences between the measurements of Hug *et al.* and those of Z-ROA are due to backward- *versus* forward-scattering, respectively.

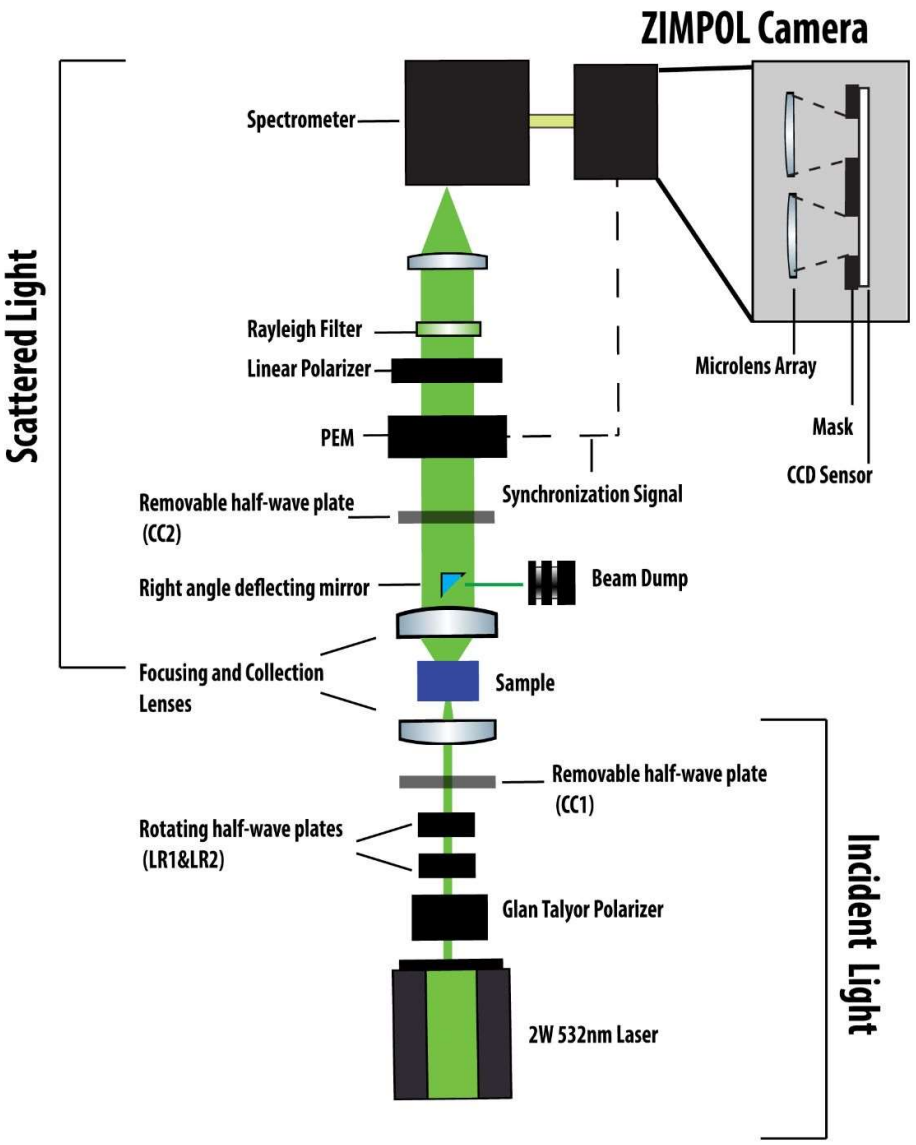

Figure 1. Schematic of the Z-ROA instrument. LR1 and LR2 are zero-order half-wave plates in custom-made rotating mounts. CC1 and CC2 are zero-order half-wave plates mounted in sliding mounts. The inset (top right) shows a schematic of the ZIMPOL camera system showing the microlens array that focuses the light onto the open (unmasked) pixel rows. The charges below the mask are shifted in synchrony with the photoelastic modulator (PEM) to sort light of different polarization states onto different rows of the CCD pixel array.

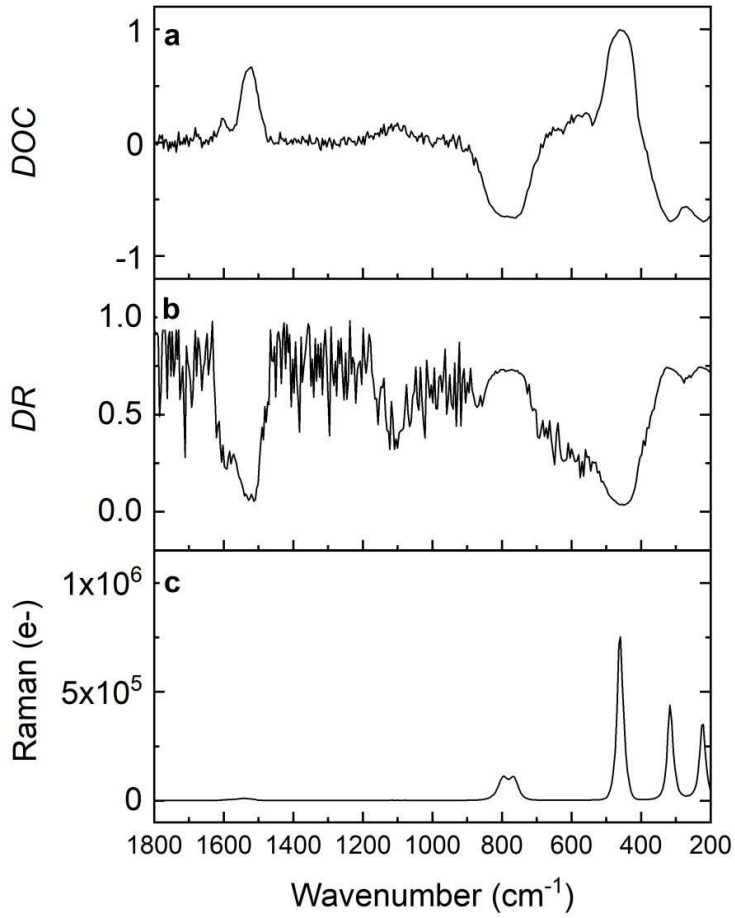

Figure 2. (a) The degree of circularity (*DOC*), (b) depolarization ratio (*DR*), and (c) Raman spectra ($I_R + I_L$) of CCl_4 measured with our Z-ROA experimental setup. These reference measurements on achiral CCl_4 give an indication of how the instrument discriminates circular (*DOC*) *versus* linear (*DR*) polarization in the scattered light.

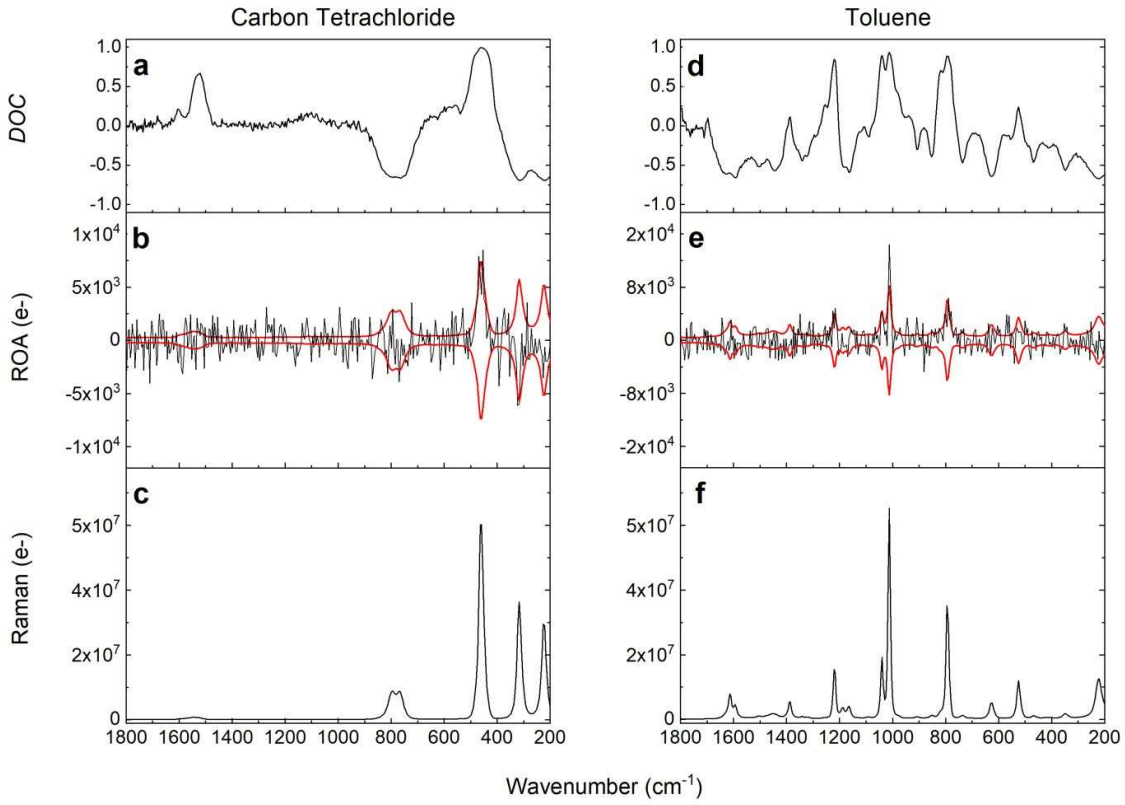

Figure 3. Control ROA measurements of achiral molecules. The left and right panels show results for CCl_4 and toluene, respectively. (a,d) *DOC* measured with incident circularly polarized light. (b,e) Spectra of the difference in scattered intensity $I_R - I_L$ (*i.e.* the ROA signal) with incident depolarized light. The expected error due to shot noise, calculated as the square root of the Raman spectra, is shown with the red line. (c,f) Spectra of the sum $I_R + I_L$ (*i.e.* the Raman signal) measured with unpolarized light. The measurements were taken with 0.5 W of laser power, 1 mL of sample volume, and roughly 2 min of measurement time, with no virtual-enantiomer correction.

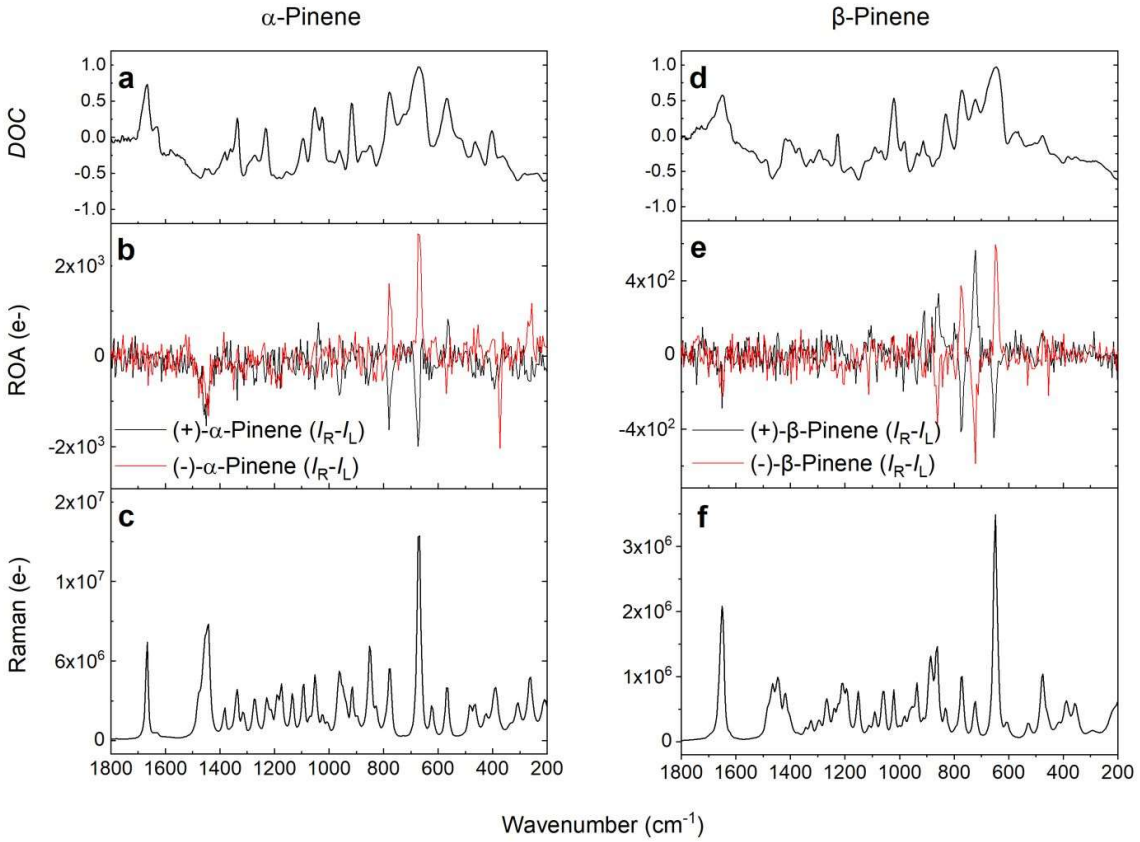

Figure 4: ROA measurements of chiral molecules with two-phase virtual enantiomer correction. The left and right panels show results for α-pinene and β-pinene, respectively. (a,d) *DOC* measured with incident circularly polarized light. (b) ROA spectra ($I_R - I_L$) for (+)-α-pinene and (−)-α-pinene. (e) ROA spectra for (+)-β-pinene and (−)-β-pinene. (c,f) Raman spectra ($I_R + I_L$) for (+)-α-pinene and (+)-β-pinene, respectively. The measurement conditions for α-pinene were 0.75 W of laser power, 1 mL of sample volume, and 40 min of measurement time. The measurement conditions for β-pinene were 1.5 W of laser power, 1 mL of sample volume, and 4 min of measurement time.

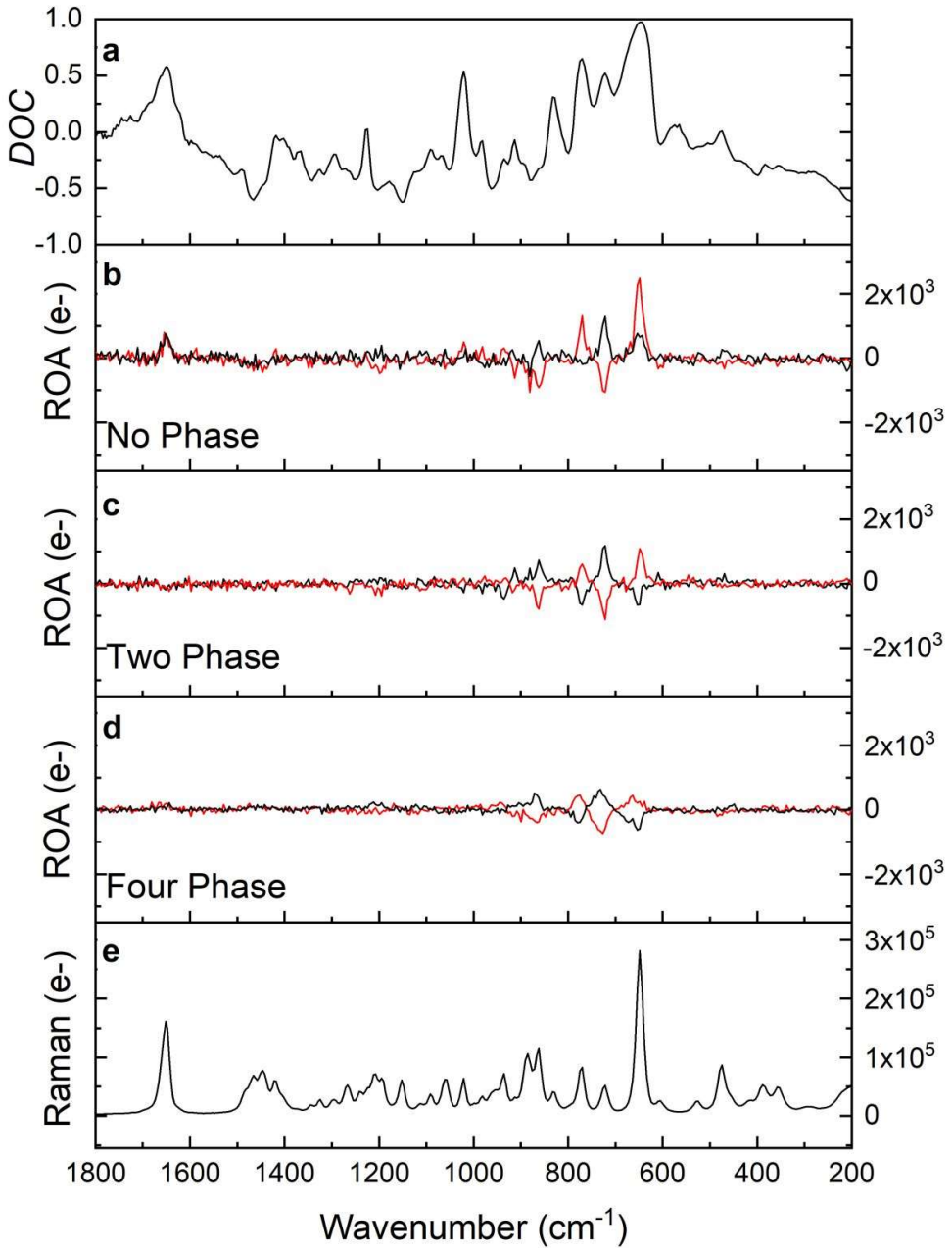

Figure 5: ROA measurements of chiral molecules with virtual enantiomer correction. (a) *DOC* of β-pinene. (b) ROA spectra ($I^R - I^L$) of (+)-β-pinene (black curve) and (−)-β-pinene (red curve) without any virtual-enantiomer correction (no phase). (c,d) ROA spectra ($I^R - I^L$) of (+)-β-pinene (black curve) and (−)-β-pinene (red curve) with two-phase and with four-phase virtual enantiomer correction, respectively. (e) Raman spectrum ($I^R + I^L$) of (+)-β-pinene. All measurements were taken with 1.5 W of incident laser power, 1 mL of sample volume, and 2, 4, and 8 min of measurement time, respectively, for no, two- and four-phase correction.